

Type of Contribution: Original Research Article

Direct observation and characterization of the generation of organic solvent droplets with and without triglyceride oil by electrospraying

Xian Zhang^{a,b,c}, Isao Kobayashi^{a,*},
Kunihiko Uemura^a, and Mitsutoshi Nakajima^{a*}

^a *Food Engineering Division, National Food Research Institute, NARO, 2-1-12,*

Kannondai, Tsukuba, Ibaraki 305-8642, Japan

^b *Graduate School of Life and Environmental Sciences, University of Tsukuba, 1-1-1,*

Tennoudai, Tsukuba, Ibaraki 305-8572, Japan

^c *School of Agricultural and Food Science, The Key Laboratory for Quality*

Improvement of Agricultural Products of Zhejiang Province,

Zhejiang A & F University, Lin'an, Hangzhou, Zhejiang, 311300, China

* Corresponding authors.

E-mails: isaok@affrc.go.jp (I. Kobayashi),

nakajima.m.fu@u.tsukuba.ac.jp (M. Nakajima)

ABSTRACT

The primary aim of this study was to investigate the generation characteristics of organic solvent droplets with and without triglyceride oil by electrospraying using single-nozzle and nozzle-array devices. The liquids used were ethanol (10 to 99.5%), ethanol (99.5%) solutions containing a triacylglyceride oil, ethyl acetate, hexane, and heptane. The droplet generation behaviors from an electrode nozzle were observed using high-speed video cameras. Unstable micro-dripping mode was observed when using ethanol (<50%), hexane, and heptane. In contrast, the stable electrospraying by cone-jet mode was achieved when using ethanol (>66.7%) and ethyl acetate. The jet diameter values mostly ranged between 10 and 20 μm , which is similar to the estimated ones. High-speed photographic observation at a frame rate of 10^6 s^{-1} demonstrated the generation of ethanol droplets at very high frequencies of 3.0×10^5 to $5.0 \times 10^5 \text{ s}^{-1}$ by breaking up the jet. The ethanol jet diameter increased with increasing the flow rate (1 to 10 mL/h). The nozzle number per device did not affect the jet diameter when the flow rate per nozzle is the same. The stable cone-jet mode was also achieved when using ethanol solution containing 0.1% triacylglyceride oil. Triacylglyceride oil droplets with diameters of about 2 μm were collected after evaporating ethanol from the droplets generated by electrospraying.

Keywords: Electrospraying; Organic solvent; Triglyceride oil; Droplet generation; Direct observation; Nozzle array

1. Introduction

Electrospraying (electrohydrodynamic spraying) is a method of liquid atomization induced by electrical force [1]. With electrospraying, liquid surface tension is balanced by electrical force at each point on the liquid surface. When electrical force and gravity force that act on a drop overcome the surface tension, the meniscus of the liquid caused the jet formation. The cone-jet leads to fission and subsequently disrupts into fine droplets due to the instability of the jet. From the energy viewpoint, liquid forms a jet when the kinetic energy of the liquid is greater than the surface energy required for creating the surface of the jet [2]. Thus, variations in normal electric stress at the apex of the meniscus, the energy gain per unit area of the liquid, and the tangential electric stress at the meniscus lateral are evaluated in the forms of electrospraying modes. When the tangential electric stress is intense enough, a cone-jet is formed [3].

Electrospray systems have the following advantages over mechanical atomizers. The droplet size can be smaller than 1 μm . The size distribution of the droplets can be nearly monodisperse [4]. The charge and size of the droplet can be easily controlled (including deflection or focusing) to some extent by adjusting the flow rate and voltage applied to the nozzle [5].

Electrospraying can be widely applied to both industrial processes and scientific instrumentations. Interest in industrial or laboratory applications has recently prompted the search for effective techniques that enable control of the processes in which droplets are involved. Electrospraying techniques are aimed at developing new drug-delivery systems, medicine production, and ingredient dosage in the cosmetic and food industries. In particular, electrospraying has recently been adapted for many applications (e.g., medical powder production [6], fine metal powder production [7], film coating [8],

electrostatic painting [9], and fuel injection [10]).

Electrospraying is often performed in typical modes. Among these modes, many studies have focused on the cone-jet mode, in which the liquid meniscus appears to have a Taylor cone [11-15]. The size distribution of the droplets produced in cone-jet mode depends on the jet diameter and the type of jet instabilities (e.g., varicose instability and kink instability) [16]. The jet diameter is a strong function of the axial distance, which may be due to solvent evaporation. Therefore, it is important to make comparisons at a fixed point below which there is negligible change in jet diameter [17]. Xie et al. [18] also developed a hypothesis explaining the characterization of particles obtained by electrospraying under various operating conditions (e.g., polymer solution flow rate, polymer concentration, and type of chemical solvent). Electrospraying are also generally performed using polar liquids (e.g., water, ethanol, glycerol, and polyethylene glycols). Ethanol has been used for understanding fundamental properties of electrospraying and as a carrier fluid for producing micro/nanoparticles [19-21]. Martin et al. [19] reported how liquid flow rate and nozzle and flat plate voltages influence the cone-jet domain for electrospraying using pure ethanol.

Droplets generated by electrospraying have potential food applications as forms of micro/nano-particles and micro/nano-dispersions. However, few electrospraying researches using food-grade materials have been conducted [22,23]. Therefore, the present work attempts to employ the electrospraying technology to generate the fine droplet consisting of organic substances. Here, we investigate the production process focusing on the type of organic solvents, the effects of device and operating conditions, high-speed camera observation of droplet generation. We also investigated the generation of droplets consisting of an organic solvent and a triacylglyceride oil as well

as the formation of triacylglyceride oil droplets by solvent evaporation from the droplets.

2. Materials and methods

2.1. Experimental setup

2.1.1. Electrode nozzle devices

Stainless-steel 24×24-mm devices with different numbers (1, 4, or 12) of electrode nozzles were designed and fabricated for this study (Fig. 1). Initially, each circular through-hole with a diameter of 600 μm on a polished metal plate was fabricated by microdrilling. Subsequently, each electrode nozzle with an inner diameter of 230 μm and a length of 13 mm was connected to the through-hole by solder bonding.

2.1.2. Electrospraying module and peripherals

Fig. 2 is a simplified schematic diagram of the experimental setup for electrospraying using electrode nozzle devices. It consists of a holder equipped with the device, a metal ring with a diameter of 100 mm as the extractor electrode, a syringe pump (Model-11, Harvard Apparatus, USA) for feeding an organic liquid, a high voltage DC power supply (KHV-U5003, Kyoshin Electric Co., Ltd., Japan) for applying an electric field to the liquid, a high-speed video camera with a maximum frame rate of $2.5 \times 10^5 \text{ s}^{-1}$ (Fastcam SA1.1, Photron Ltd., Japan) or 10^6 s^{-1} (HyperVision HPV-1, Shimadzu Co., Japan), and a metal halide light source (LS-M210, Sumita Optical Glass, Inc., Japan).

2.2. Chemicals and solution preparation

The organic solvents used in this study are ethanol (purity 99.5%, Nacalai Tesque, Inc., Japan), *n*-hexane (Wako Pure Chemical Industries Ltd.), *n*-heptane (Wako Pure Chemical Industries Ltd.), and ethyl acetate (Wako Pure Chemical Industries Ltd.). Ethanol solutions with a concentration of 10 to 99.5% were prepared by mixing 99.5% ethanol with deionized and filtered water (Milli-Q water). Refined soybean oil (Wako Pure Chemical Industries Ltd.) as a model long-chain triglyceride, and medium-chain triglyceride (MCT) oil (MCT-7, Taiyo Kagaku Co. Ltd., Japan) were also dissolved in 99.5% ethanol at a concentration of 0.1% and a room temperature of 25 °C.

2.3. *Experimental procedure*

Prior to the electrospraying experiments, an electric nozzle device was fixed in the holder, and the tip of each electrode nozzle was positioned at 10 mm over the ring grounding electrode. Each liquid was contained a 10-mL glass syringe and was introduced into the module using a syringe pump at a liquid flow rate (Q_L) of 1 to 10 mL/h for the single nozzle device, 6 mL/h for the 4-nozzle device, and 18 mL/h for the 12-nozzle device. Next, the liquid was injected from the nozzle tip under positive DC voltage (V_{DC}) (3.7 to 14 kV) in order to generate organic solvent droplets. At that moment, the nozzle tip was positively electrified, while the ring was grounded. All experiments were conducted at 25 °C. Electrospraying characteristics were microscopically observed using a high-speed video camera at 9000 to 15000 fps for Fastcam SA1.1 or 10^6 fps for HyperVision HPV-1.

Image-analysis software (WinRoof version 5.6, Mitani Co., Japan) was used to measure the diameters of the droplets on the images captured during experiments. The mean diameter of the droplets generated under each condition was determined using the

measured data of 30 droplets.

2.4. Determination of viscosity, electrical conductivity, and surface tension

A Sine-wave vibroviscometer (SV-10, A&D Co., Ltd., Japan) was used to determine the absolute viscosities of the liquids (defined as the ratio of liquid viscosity to liquid density). The electrical conductivities of the liquids were measured using a conductivity electrode (Model 9382-10D, Horiba Ltd., Japan). The surface tensions of the liquids were determined using a fully automatic surface tensiometer (CBUP-Z, Kyowa Interface Science Co., Ltd, Japan) that adopts the Wilhelmy Plate method. The contact angles of the liquids to a stainless-steel plate were determined using a fully automatic interfacial tensiometer (PD-W, Kyowa Interface Science Co., Ltd, Japan). Measurements of liquid viscosity, electrical conductivity, surface tension, and contact angle were repeated at least three times at 25 °C; their mean values are presented in Table 1.

3. Results and discussion

3.1. Effect of organic solvent type

3.1.1. Electrospraying characteristics

Electrospraying experiments were first conducted using four different organic solvents. Fig. 3 depicts microscopic snapshots of electrospraying from a single nozzle. The Q_L applied here was 1 mL/h for ethanol, hexane, and heptane, and 6 mL/h for ethyl acetate. Ethanol (99.5%) ejected from the nozzle tip formed a stable cone and jet (cone-jet mode) at a V_{DC} of 3.7 kV (Fig. 3a). Due to electrostatic force, this jet broke up into droplets (see Sect. 3.2). The use of ethyl acetate also resulted in the formation of

the cone-jet mode at a V_{DC} of 3.7 kV (Fig. 3b). It should be noted that ethyl acetate rapidly evaporated from the nozzle tip at a Q_L of 1.5 mL/h, as the viscosity of ethyl acetate is about one-third of that of ethanol. The boiling point of ethyl acetate (77.2 °C) is similar to that of ethanol (78.4 °C). By contrast, heptane and hexane ejected from the nozzle irregularly formed large droplets with diameters of >100 μ m nearby the cone tip (microdripping mode) at a Q_L of 6.5 kV for hexane and 5.8 kV for heptane (Fig. 3c and d). The difference in these electrospraying characteristics could be explained using the properties of the organic solvents (Table 1). There was unpronounced difference in the surface tension of the organic solvents. The viscosity values of hexane and heptane were similar to that of ethyl acetate, while remarkable solvent evaporation was not observed for hexane and heptane ejected from the nozzle tip. These results indicate that their surface tension and viscosity are not dominant factors affecting the electrospraying modes in this case. The solvent conductivity was appreciably influenced by solvent type. The conductivities of ethanol and ethyl acetate were at least two orders of magnitude greater than those of hexane and heptane. Earlier studies reported that liquid conductivity plays a critical role in electrospraying characteristics, and that a stable cone-jet mode can be obtained using liquids with a conductivity of 10^{-7} to 10^{-2} S/m [12,16,21]. It is currently assumed that liquids can be electrosprayed in cone-jet mode at conductivities of 10^{-4} to 10^{-8} S/m [5]. The conductivities of ethanol and ethyl acetate are thus considered to be appropriate for stable electrospraying in cone-jet mode.

3.1.2. Estimating jet diameter

To achieve stable electrostatic atomization, the electrical relaxation time ($t_e = \beta\epsilon_0 / K_L$) must be much smaller than the hydrodynamic time ($t_h = l_j d_j^2 / Q_L$) [24]:

$$\frac{\beta \epsilon_0}{K_L} \ll \frac{l_j d_j^2}{Q_L}, \quad (1)$$

where β is the relative permittivity, ϵ_0 is the permittivity of free space (8.854×10^{-12} F/m), K_L is the electrical conductivity, and l_j and d_j are the jet length and diameter. Hence, the dimensionless viscous parameter (δ_m) is defined by Ganan-Calvo et al. [25] as

$$\delta_m = \sqrt[3]{\frac{\rho_L \epsilon_0 \gamma^2}{K_L \eta_L^3}}, \quad (2)$$

where ρ_L is liquid density, γ is surface tension, and η_L is viscosity of liquid. For $\delta_m \gg 1$, the jet diameter (d_j) in stable cone-jet mode can be estimated by [25]:

$$d_j \approx \sqrt[6]{\frac{\rho_L \epsilon_0 Q_L^3}{\gamma K_L}} \quad (3).$$

Substituting the physical values of ethyl acetate in Eq. 2 indicates that δ_m for the ethyl acetate is $\gg 1$ and therefore, d_j is 15 μm at a Q_L of 6.0 mL/h. Conversely, for $\delta_m \ll 1$, d_j is given by [25]:

$$d_j \approx \sqrt[3]{\frac{(\beta - 1)^{1/2} Q_L \epsilon_0}{K_L}}, \quad (4).$$

Substituting the values of 99.5% ethanol in Eq. 4 yields a d_j of 8 μm at a Q_L of 1.5 mL/h. Based on these results, the measured jet diameters of ethyl acetate and ethanol are similar to the estimated values.

3.1.3. High-speed camera analysis of droplet generation by cone-jet mode

A high-speed camera with a maximum frame rate of 10^6 s^{-1} was used to investigate

droplet generation of 99.5% ethanol using the single-nozzle device. During electrospraying, the liquid formed a conical meniscus at the nozzle tip, and the jet ejected from the nozzle broke up into uniformly sized droplets. High-speed photographic observation (Fig. 4) indicated that fine droplets were generated at remarkably high frequencies of 3.0×10^5 to $5.0 \times 10^5 \text{ s}^{-1}$ under the Q_L of 1.0 mL/h and the V_{DC} of 3.7 kV. In stable electrospraying, the Rayleigh law is defined as [26]

$$\frac{d_d}{2d_j} = 1.89 \quad , \quad (5)$$

where d_d is the droplet diameter. The d_d calculated using Eq. 5 was 14 μm , which is similar to the d_d measured from the experiment.

3.2. *Effect of ethanol concentration and flow rate*

Ethanol concentration affects many physical properties of a liquid (e.g., viscosity, density, surface tension, and conductivity); therefore, it is expected to have a great influence on electrospraying characteristics. Single-phase ethanol with a concentration of 10 to 99.5 wt% was made to flow through a single electrode nozzle, 4 electrode nozzles, and 12 electrode nozzles (Fig. 1). The flow rates of all nozzles were the same; 1.5 mL/h for the single nozzle, 6 mL/h for the 4-nozzle array, 18 mL/h for the 12-nozzle array. The V_{DC} values were 4.2 kV for the single nozzle, 9.0 to 11.0 kV for the 4-nozzles, and 12.5 to 14.0 kV for the 12-nozzles. Figure 5a shows the influence of ethanol concentration on the droplet/jet diameter obtained by electrospraying. The influence of ethanol concentration on the surface tension, conductivity, and viscosity of ethanol are also presented in Fig. 5b, c. The processed liquids exhibited microdripping at concentrations of 50% or less (Fig. 5a), which be mainly due to higher surface tension

(Fig. 5b). This may have prevented electro spraying in the stable cone-jet mode at the flow rates and voltages applied here. Electrostatic atomization in cone-jet mode is difficult with liquids containing a high proportion of water [14,27,28] unless specified conditions (e.g., flow rate, surrounding atmosphere, and conductivity) are met [28,29]. The use of ethanol solutions with a concentration of 67% or higher exhibited electro spraying in the cone-jet mode with a narrower jet diameter ranging between 10 and 20 μm (Fig. 5a), indicating that the diameter of ethanol droplets generated in this cone-jet mode decreased slowly with increased the ethanol concentration. The stable cone-jet mode was achieved at surface tensions of 22 to 27 mN/m, conductivities of 1.6×10^{-7} to 8.3×10^{-7} S/m, and viscosities of 0.8 to 1.8 mPa s. It should be noted that the viscosity values of ethanol for the microdripping mode were similar to those for the cone-jet mode (Fig. 5b). The results in Fig. 5a also demonstrated that the resultant jet (and droplet) diameter was hardly affected by the nozzle number at an ethanol concentration of 67% or higher.

Jayasinghe et al. [30] suggested that the flow rate has to be minimized to obtain the finest droplets. However, no stable cone can be formed at flow rates being too low. The values of β , ϵ_0 , and K_L in Eq. 4 do not change for ethanol, and the jet diameter of ethanol increases monotonically with increased flow rates. Among the various parameters, flow rate is the simplest and most effective variable for controlling jet diameter. Therefore, to analyze the influence of 99.5% ethanol flow rate, the applied voltage was kept constant throughout the investigation at 4.4 kV by using the single-nozzle device. Ethanol that ejected from the nozzle tip formed the cone-jet mode at all the flow rates (1 to 10 mL/h). The cone depth, defined as distance from the nozzle tip to the apex of the cone, increased gradually from 150 to 670 μm as the flow rate

increased (Fig. 6a). The ethanol flow rate also affected the jet diameter which ranged between 9.0 and 16.1 μm (Fig. 6b). The jet diameter increased slowly with increasing the flow rate in its range of 2 to 10 mL/h, whereas the slope of the jet diameter became higher at the low flow rates of < 2 mL/h.

3.3. *Electrospraying characteristics of ethanol solution containing triacylglyceride oil*

3.3.1. *Effects of oil type and flow rate*

Electrospraying an ethanol solution containing MCT (0.1%) or soybean oil (0.1%) formed a stable cone-jet using the single nozzle at a Q_L of 1 mL/h and a V_{DC} of 4.0 kV (Fig. 6). The effect of the flow rate of the ethanol solutions on the cone depth and jet diameter is also shown in Fig. 6. The values of the liquid properties are listed in Table 1. The shape and the wettability of the nozzle material can pronouncedly influence the shape of the cone formed, the stability of the jet, and the electrospraying mode [30,31]. The contact angle is an indicator of the wettability of a liquid to the nozzle surface. The wettability of the liquids became poor with increased contact angle on the stainless-steel plate. The static contact angle of 99.5 wt% ethanol to the stainless-steel plate was $<10^\circ$, indicating that the nozzle surface is easily wetted by ethanol during electrospraying. The static contact angle of MCT on the stainless-steel plate was 20° , and that of soybean oil was 15° . The formed cone and jet of the ethanol solution containing soybean oil were somewhat larger (Fig. 6), which may be attributed to its higher wettability to the nozzle surface.

At the Q_L of 1 mL/h, the jet diameter was 13 μm for MCT and 18 μm for soybean oil. The jet diameters of the ethanol solutions increased with increasing the Q_L in ranges of >2 mL/h or more for MCT and >1 mL/h for soybean oil. The slope of the lines in Fig.

6b became greater between 1 and 2 mL/h for MCT and 0.5 and 1 mL/h for soybean oil. The jet diameters estimated by Eq. 4 that increased with increasing Q_L agreed with the measured results.

3.3.2. *Optical microscopy of triglyceride oil droplets*

Under adequate electrospray condition, droplet relics were collected by swiftly moving a glass slide below the ring ground electrode or over the ring ground electrode. This collection procedure was repeated at least twice. Soon after deposition, the collected droplet relics were analyzed using optical electron microscopy (Leica DMIRM, Leica Microsystems Wetzlar GmbH, Germany). The jet was confirmed to break up into droplets above the ground electrode (Fig. 7a and c). With increasing the distance between the nozzle tip and the glass slide, ethanol evaporated more from droplets, and the size of the collected droplets decreased. The average diameters of the resultant triglyceride oil droplets were about 2 μm , which is reasonable considering the oil concentration in ethanol solution.

4. Conclusions

The results have demonstrated that successful electrospraying in cone-jet mode can be achieved when using organic solvents (especially ethanol) with liquid conductivities of $>10^{-8}$ S/m and applying appropriate V_{DC} . The electrospraying behaviors were affected by ethanol concentration as well. High-speed photographic observation demonstrated that the jet formed by electrospraying broke down into fine 99.5% ethanol droplets at a maximum generation frequencies of $5 \times 10^5 \text{ s}^{-1}$. The jet diameter was affected by the type and composition of organic solvents and increased with increasing Q_L . The jet diameter

obtained from experimentation was similar to the estimated jet diameter. The successful cone-jet mode was achieved using the 4-nozzle and 12-nozzle devices when the Q_L per nozzle was the same. This finding is useful for improving low droplet productivity in electrospraying. Fine triglyceride oils with diameters of about 2 μm were also obtained by electrospraying of ethanol solution containing triglyceride oils and subsequent solvent evaporation from the generated droplets. This combined process could be applicable for forming a thin edible oil layer in foods and pharmaceuticals.

Acknowledgements

The authors appreciate Dr. Yong-Zhong Du for his valuable comments on the manuscript. The authors also thank Dr. Takashi Kuroiwa and Dr. Ai Mey Chuah for fruitful discussion.

References

- [1] R. Bocanegra, D. Galan, M. Marquez, I.G. Loscertales, A. Barrero, Multiple electrosprays emitted from an array of holes, *J. Aerosol Sci.* 36 (2005) 1387.
- [2] N.R. Lindblad, J.M. Schneider, Production of uniform-sized droplets, *J. Sci. Instrum.* 42 (1965) 635.
- [3] L.T. Cherney, Structure of Taylor cone-jets: limit of low flow rates, *J. Fluid Mech.* 378 (1999) 167.
- [4] K. Okuyama, I.W. Lenggoro, Preparation of nano particles via spray route, *Chem. Eng. Sci.* 58 (2003) 537.
- [5] A. Jaworek, Micro- and nanoparticles production by electrospraying, *Powder Technol.* 176 (2007) 18.
- [6] A. Gomez, D. Bingham, L.D. Juan, K. Tang, Production of protein nanoparticles by Electrospray drying, *J. Aerosol Sci.* 29 (1998) 561.
- [7] M. Lohmann, H. Beyer, A. Schmidt-Ott, Size and charge distribution of liquid metal electrospray generated particles, *J. Aerosol Sci.* 28 (1993) S349.
- [8] P. Miao, W. Balachandran, P. Xiao, Formation of ceramic thin films using Electrospray in cone-jet mode. Conference Record of the IEEE Industry Applications Conference, 4 (1999) 2487.
- [9] J. Dominick, A. Scheibe, Q. Ye, The electrostatic spray painting process with high-speed rotary bell atomizers: influences of operating conditions and target geometries. Ninth international conference on liquid atomization and spray systems, Sorrento, Italy, 13-17 July, 2003.
- [10] S.A. Kaiser, D.C. Kyritsis, M.B. Long, A. Gomez, "Hissing" electrospray and combustion at the mesoscale. Ninth international conference on liquid atomization

and spray systems, Sorrento, Italy, 13-17 July, 2003.

[11] C.H. Chen, M.H.J. Emond, E.M. Kelder, B. Meester, J. Schoonman, Electrostatic sol-spray deposition of nanostructured ceramic thin films, *J. Aerosol Sci.* 30, (1999) 959.

[12] A.M. Ganan-Calvo, The size and charge of droplets in the electrospraying of polar in the cone jet mode, and the minimum droplet size, *J. Aerosol Sci.* 25 (1994) 309.

[13] R.P.A. Hartman, J.P. Borra, D.J. Brunner, J.C.M. Marijissen, B. Scarlett, The evolution of electrohydrodynamic sprays produced in the cone-jet mode, a physical model. *J. Electrosta.* 47 (1999) 143.

[14] K. Tang, A. Gomez, Generation of monodisperse water droplets from electrospray in a corona-assisted cone-jet mode, *J. Colloid Interface Sci.* 175 (1995) 326.

[15] K. Tang, A. Gomez, Monodispersity electrosprays of low electric conductivity liquids in the cone-jet mode, *J. Colloid Interface Sci.* 184 (1996) 500.

[16] R.P.A. Hartman, D.J. Brunner, D.M.A. Camelot, J.C.M. Marijissen, B. Scarlett, Jet break-up in electrohydrodynamic atomization in the cone-jet mode, *J. Aerosol Sci.* 31 (2000) 65.

[17] S.N. Jayasinghe, M.J. Edirisinghe, Effect of viscosity on the size of relics produced by electrostatic atomization, *J. Aerosol Sci.* 33 (2002) 1379.

[18] J. Xie, J.C.M. Marijissen, C.H. Wang, Microparticles developed electrohydrodynamic atomization for the local delivery of anticancer drug to treat C6 glioma in vitro, *Biomat.* 27 (2006) 3321.

[19] S. Martin, A. Perea, P.L. Garcia-Ybarra, I.L. Castillo, Effect of the collector voltage on the stability of the cone-jet mode in electrohydrodynamic spraying, *J. Aerosol*

362 Sci. 46 (2012) 53.

363 [20] M.A.T. Cardoso, M. Talebi, P.A.M.H. Soares, C.U. Yurteri, J.R. van Ommen,
 364 Functionalization of lactose as a biological carrier for bovine serum albumin by
 365 electrospraying, Intl. J. Pharm. 414 (2011) 1.

366 [21] F. Lijo, E. Marsano, C. Vijila, R.S. Barhate, V.K. Vijay, S. Ramakrishna, V. Thavasi,
 367 Electrospun polyimide/titanium dioxide composite nanofibrous membrane by
 368 electrospinning and electrospraying, J. Nanosci. Nanotechnol. 11 (2011) 1154.

369 [22] M.K.I. Khan, M.A.I. Schutyser, K. Schron, R. Boom, The potential of
 370 electrospraying for hydrophobic film coating on foods, J. Food Eng. 108 (2012)
 371 410.

372 [23] M.K.I. Khan, L.H. Mujawar, M.A.I. Schutyser, K. Schron, R. Boom, Deposition of
 373 thin lipid films prepared by electrospraying, Food Bioprocess Technol. (2012)
 374 doi:10.1007/s11947-012-0974-7

375 [24] S.N. Jayasinghe, M.J. Edirisinghe, Electrostatic atomization of a ceramic
 376 suspension, J. Eur. Ceram. Soc. 24 (2004) 2203.

377 [25] A.M. Ganan-Calvo, J. Davila, A. Barrero, Current and droplet size in the
 378 electrospraying of liquids. Scaling laws, J. Aerosol Sci. 258 (1997) 249.

379 [26] L. Reyleigh, On the instability of jets, Proc. London Math. Soc. 10 (1878) 4.

380 [27] D.P.H. Smith, The electrohydrodynamic atomization of liquids, IEEE Transactions
 381 on Industrial Applications, IA-22 (1986) 527.

382 [28] J.P. Borra, Y. Tombette, P. Ehouarn, Influence of electric field profile and polarity
 383 on the mode of EHDA related to electric discharge regimes, J. Aerosol Sci. 30
 384 (1999) 963.

385 [29] A. Jaworek, A. Krupa, Classification of the modes of EHD spraying, J. Aerosol Sci.

386 30 (1999) 873.

387 [30] S.N. Jayasinghe, M.J. Edirisinghe, Electrically forced jets and microthreads of high

388 viscosity dielectric liquids, J. Aerosol Sci. 35 (2004) 233.

389

390

391 Table 1 Surface tension, conductivity, and viscosity of organic solvent solutions with
 392 and without triacylglyceride oil used for electrospraying.

393

Solution type	Surface tension (mN/m)	Conductivity (S/m)	Viscosity (mPa s)
Ethanol	22.2	1.6×10^{-5}	0.83
Ethanol (0.1% MCT)	22.0	1.7×10^{-5}	0.78
Ethanol (0.1% soybean oil)	22.2	9.0×10^{-6}	0.82
Ethyl acetate	23.4	$<1 \times 10^{-7}$	0.45
Hexane	18.3	$<1 \times 10^{-13}$	0.32
Heptane	19.7	$<1 \times 10^{-9}$	0.41

394

395

Figure captions

Fig. 1 Schematic illustrations of stainless-steel devices with different numbers (1, 4, and 12) of electrode nozzle. (a) Single-nozzle device. (b) 4-nozzle device. (c) 12-nozzle device.

Fig. 2 Schematic representation of the setup for electrospraying.

Fig. 3 Typical electrospraying behaviors of different organic solvents: (a) ethanol, (b) ethyl acetate, (c) hexane, and (d) heptane. Each liquid was ejected using a single nozzle. Scale bars are 100 μm .

Fig. 4 Typical image of stable cone-jet mode and generation of 99.5% ethanol droplets. This image was taken at a frame rate of 10^6 s^{-1} .

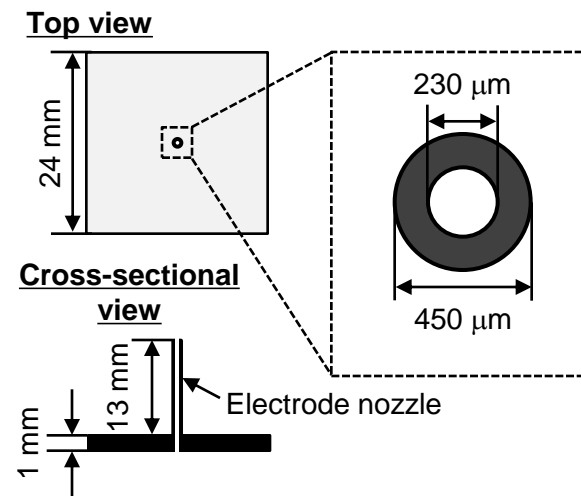
Fig. 5 Variations in jet and droplet diameters (a), surface tension and viscosity (b), and conductivity (c) as a function of ethanol concentration.

Fig. 6 Variations in cone depth (a) and jet diameter (b) as a function of flow rate. The images in (c and d) are examples of electrospraying of ethanol solutions each containing a triglyceride oil. The cone depth and jet diameter are defined in (c).

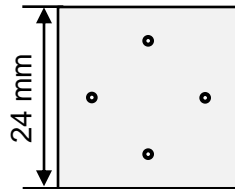
Fig. 7 Optical micrographs of ethanol droplets containing 0.1% MCT (a and b) or 0.1% soybean oil (c and d) collected on a glass slide. The distance in (a and c) was 0.5 cm

420 below the ring electrode, and that in (b and d) was 2 cm over the ring electrode. Scale
421 bars are 10 μm .

(a) Single nozzle



(b) 4 nozzles



(c) 12 nozzles

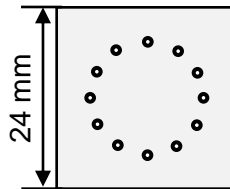


Fig. 1

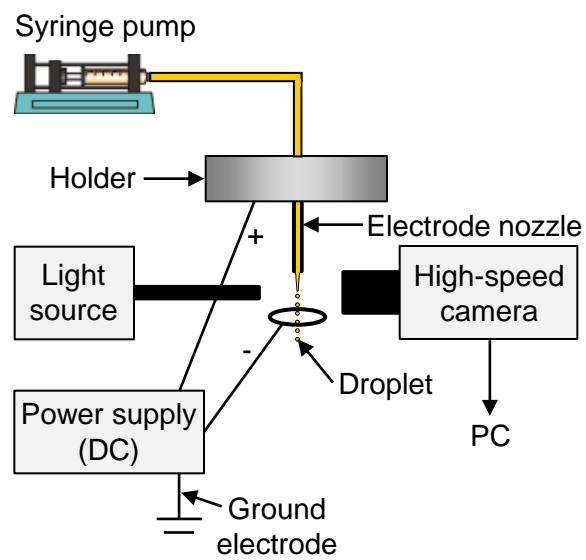


Fig. 2

Zhang *et al.*

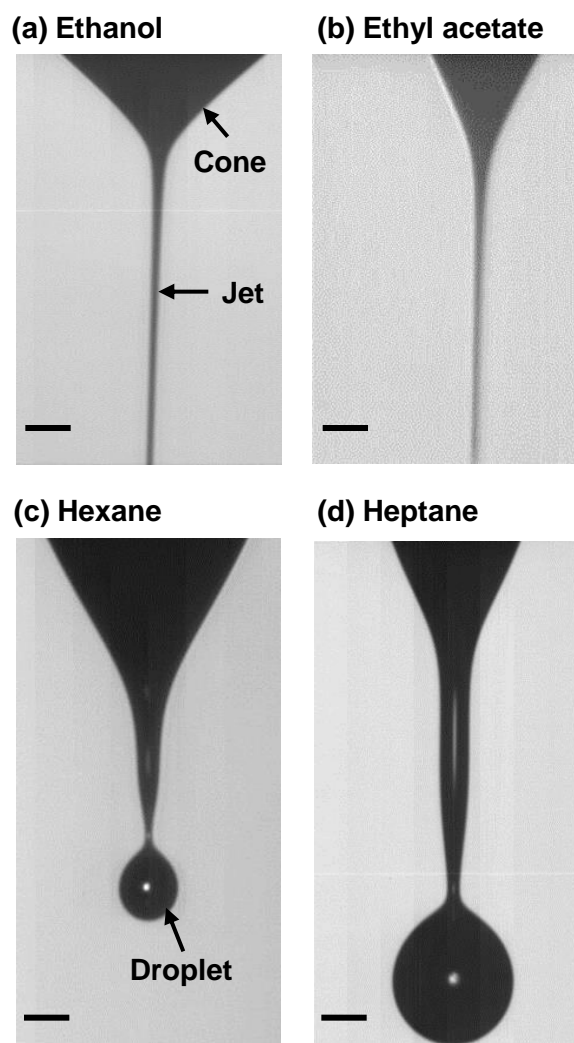


Fig. 3

Zhang *et al.*

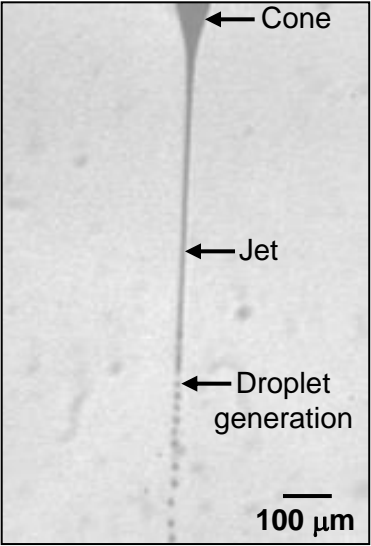


Fig. 4

Zhang *et al.*

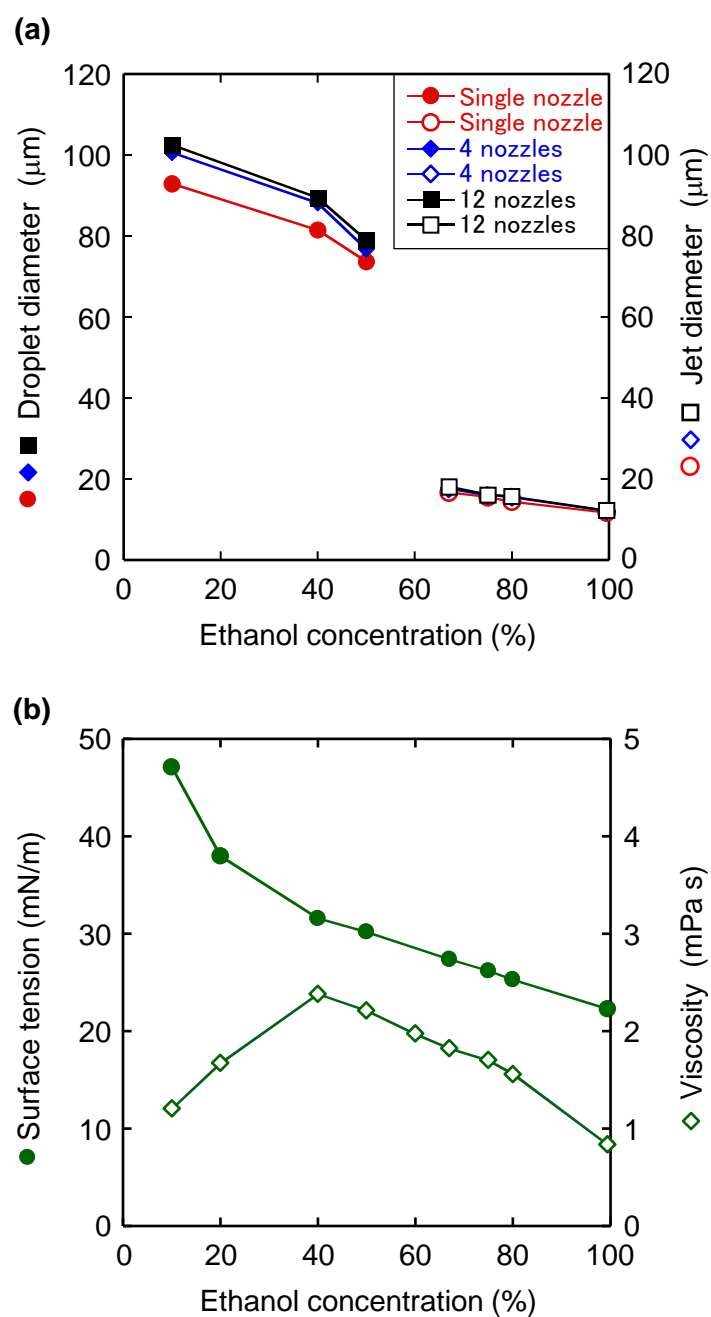


Fig. 5

Zhang *et al.*

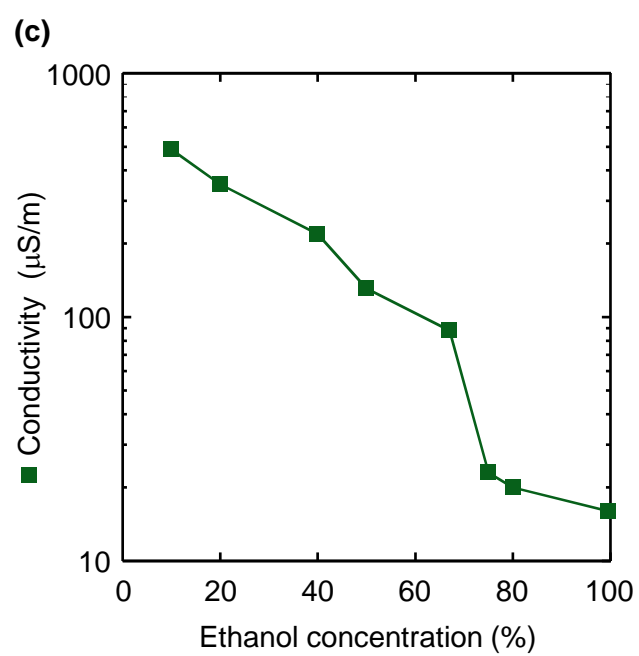


Fig. 5 (Cont.)

Zhang *et al.*

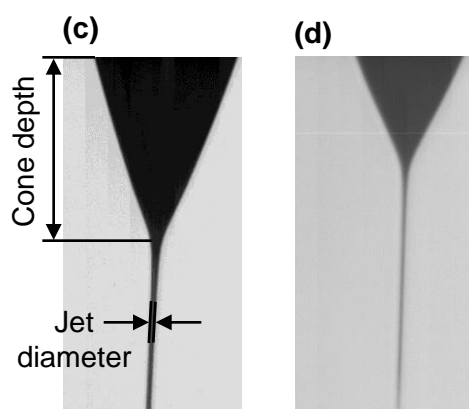
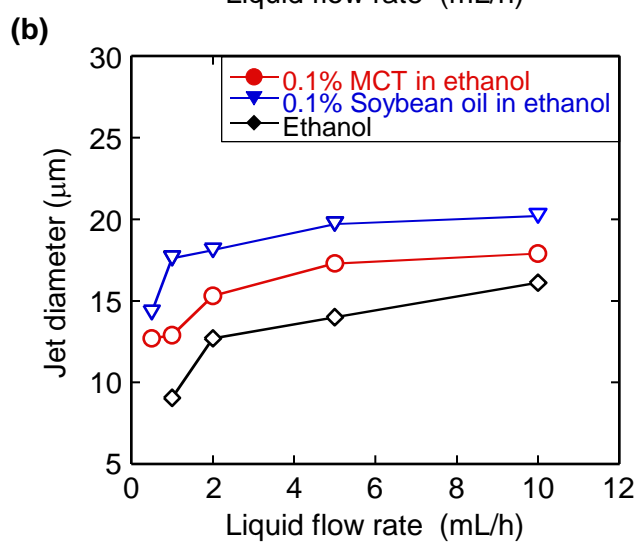
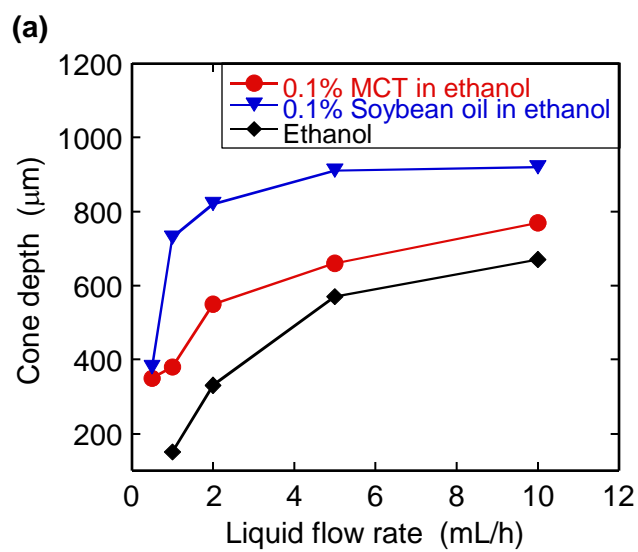


Fig. 6

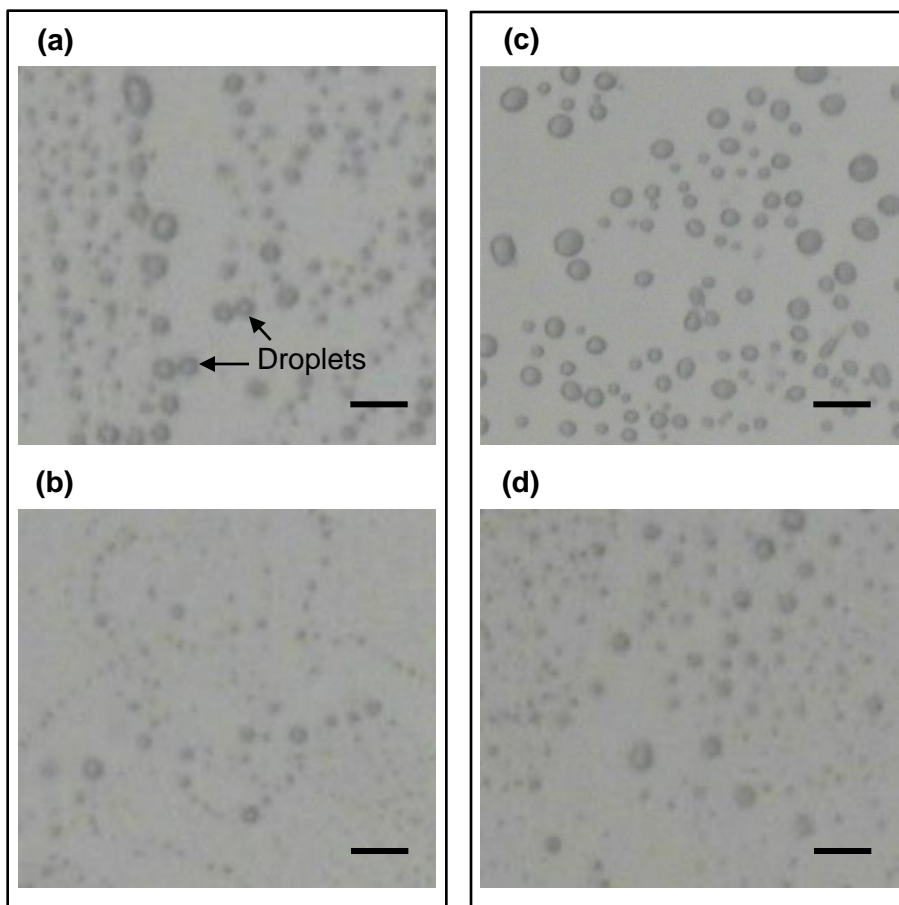


Fig. 7

Zhang *et al.*